0026-895X/95/040787-11$3.00/0

MOLECULAR PHARMACOLOGY, 47:787–797 (1995).

Mastoparan Increases the Intracellular Free Calcium Concentration in Two Insulin-Secreting Cell Lines by Inhibition of ATP-Sensitive Potassium Channels

GEOFFREY T. EDDLESTONE,[1] MITSUHISA KOMATSU, LINMING SHEN, and GEOFFREY W. G. SHARP

Department of Pharmacology, College of Veterinary Medicine, Cornell University, Ithaca, New York 14850

Received April 28, 1994; Accepted January 31, 1995

SUMMARY

The mechanisms underlying mastoparan-induced elevation of the intracellular free calcium concentration ($[Ca^{2+}]_i$) were investigated in the insulin-secreting cell lines RINm5F and HIT. In both cell types, micromolar concentrations of mastoparan induced a prompt increase of $[Ca^{2+}]_i$, measured as an increase in fura-2 fluorescence. This response was dependent on extracellular calcium entry and was suppressed by organic calcium channel blockers; the increase of $[Ca^{2+}]_i$ caused by high glucose concentrations or tolbutamide was not enhanced by mastoparan. These data indicate the involvement of voltage-dependent calcium channels and suggest that depolarization, rather than a direct effect on the channels, mediates the response to mastoparan. This proposition was supported by the observation that whole-cell calcium currents measured using the nystatin-permeabilized patch technique were not affected by mastoparan. Mastoparan-induced depolarization was observed using the potentiometric indicator bis-oxonol, and it was shown not to be additive with the depolarization induced by high glucose concentrations or tolbutamide. The mechanism underlying mastoparan-induced depolarization was identified in single-channel patch-clamp experiments, where it was shown that mastoparan caused closure of ATP-sensitive potassium channels [K(ATP) channels] in cell-attached and excised membrane patches. Responsiveness to mastoparan in excised patches demonstrated the membrane-delimited character of K(ATP) channel inhibition. The observation that the response persisted in the absence of exogenous GTP and in the presence of 250 μM GDP or guanosine-5′-*O*-(2-thio)diphosphate suggested that this effect is not mediated via enhancement of G protein activity. Partial suppression of channel activity by mastoparan did not prevent the action of tolbutamide, which fully suppressed the remaining activity in excised patches. In summary, the increase of $[Ca^{2+}]_i$ in the insulin-secreting tumor cell lines RINm5F and HIT in response to mastoparan is mediated via G protein-independent suppression of K(ATP) channel activity, cell depolarization, and activation of voltage-dependent calcium channels.

Mastoparan, an amphiphilic tetradecapeptide component of wasp venom (1), has pleiotropic effects on a variety of cell types. Enhanced secretion occurs in response to mastoparan in mast cells (2–4), neutrophils (5), pituitary lactotrophs (6), adrenal chromaffin cells (7), PC-12 cells (8), pulmonary alveolar cells (9), platelets (10, 11), and insulin-secreting cells, both primary cells (12–14) and cell lines (15, 16). Among biochemical mechanisms implicated in the secretory responses is facilitation of the activity of phospholipase A_2 (2, 9, 12, 13, 17) and of phospholipase C (3–5, 8, 18, 19). However, mastoparan may reduce membrane polyphosphoinositide breakdown, either by suppression of phospholipase C (20) or by direct interaction of the venom component with polyphosphoinositide, reducing its susceptibility to phospholipase C (21). Mastoparan has also been implicated in both stimulation (11) and suppression (9, 20) of adenylyl cyclase. Additionally, mastoparan binds calmodulin with a 1:1 stoichiometry (22) and inhibits its activity (23). Mastoparan increases DNA synthesis (17) and enhances nucleotide exchange at both heterotrimeric (4, 24–26) and low molecular weight (27) G proteins. Lytic effects of mastoparan have also been reported (6, 28, 29).

Intracellular free calcium is a critical mediator in stimulus-secretion coupling in many cell types, including insulin-secreting cells (30). Although mastoparan-induced secretion is accompanied by elevation of $[Ca^{2+}]_i$ in insulin-secreting cells and other cell types (5, 8, 9, 13, 16), several studies have demonstrated that secretion is not dependent upon elevation

This work was supported by National Institutes of Health Grants R01-DK39652 and R01-DK42063.

[1] Current address: Masonic Medical Research Laboratory, 2150 Bleecker Street, Utica, NY 13501–1787.

ABBREVIATIONS: $[Ca^{2+}]_i$, intracellular calcium concentration; K(ATP) channel, ATP-sensitive potassium channel; KRB, Krebs-Ringer bicarbonate; HEPES, 4-(2-hydroxyethyl)-1-piperazineethanesulfonic acid; EGTA, ethylene glycol bis(β-aminoethyl ether)-*N,N,N′,N′*-tetraacetic acid; GDPβS, guanosine-5′-*O*-(2-thio)diphosphate; PKC, protein kinase C.

of $[Ca^{2+}]_i$. Thus, for rat islet β cells (14), RINm5F cells (16), mast cells (10), and adrenal chromaffin cells (31), it was concluded that the peptide may act at a late phase in stimulus-secretion coupling, distal to the step requiring increased $[Ca^{2+}]_i$. Furthermore, the observation that mastoparan-induced secretion from permeabilized rat islet β cells (14) and platelets (11) is partially suppressed by GDPβS reinforces the proposal that one target for mastoparan action is the putative exocytotic G protein G_o (11, 14, 16). These data indicate that mastoparan interacts with the stimulus-secretion pathway at more than one locus. The present study was carried out to investigate the mechanism underlying the mastoparan-induced rise in $[Ca^{2+}]_i$.

Nutrient secretagogues and the antidiabetic sulfonylureas elevate $[Ca^{2+}]_i$ in insulin-secreting cells by depolarization and activation of voltage-dependent calcium channels (32), principally of the L type (33); cell depolarization results from suppression of the predominant potassium permeability, provided by the K(ATP) channel (32, 34). The results of the present investigation demonstrate that, in common with these recognized secretagogues, mastoparan also suppresses K(ATP) channel activity and causes depolarization, implicating this pathway in mastoparan-induced $[Ca^{2+}]_i$ elevation. As reported previously, however, the mastoparan-induced rise in $[Ca^{2+}]_i$ does not appear to contribute to the secretory response (16).

Experimental Procedures

Cell culture. Cells of the insulin-secreting tumor cell lines HIT and RINm5F were used in this study, the former at passages 65–80 and the latter at passages 57–65. Cell lines were maintained at 37° in monolayer culture in plastic culture flasks, in HCO_3-buffered RPMI 1640 culture medium (with 10% fetal bovine serum, 100 μg/ml streptomycin, and 100 units/ml penicillin), and were passaged once each week, as described previously (16). For fluorescence measurements cells were seeded at an initial density of 250×10^3 cells/ml and used 3–5 days later. The cells were collected from the culture flasks after a brief trypsin/EDTA treatment, transferred to RPMI 1640 medium with 5% fetal bovine serum at pH 7.4, and maintained at room temperature before loading. For electrophysiological investigations cells were plated onto glass microscope coverslips at a density of 500×10^3 cells/ml and used in experiments 3–5 days later.

Fura-2 fluorescence measurement of $[Ca^{2+}]_i$. Before loading with fura-2, the cell suspension was centrifuged and resuspended in KRB buffer (129 mM NaCl, 5 mM $NaHCO_3$, 4.8 mM KCl, 1.2 mM KH_2PO_4, 1.0 mM $CaCl_2$, 1.2 mM $MgSO_4$, 10 mM HEPES, pH adjusted to 7.4 with NaOH). Bovine serum albumin was added at 0.1% and glucose at 0.2 or 2.8 mM, the former usually for HIT cells and the latter for RINm5F cells. For loading with fura-2, cell density was adjusted to 4×10^6 cells/ml and the KRB buffer was supplemented with 0.25 mM sulfinpyrazone and 1 μM fura-2/acetoxymethyl ester; the cell suspension was then incubated in a shaking waterbath at 37° for 30 min. Fura-2-loaded cells were washed three times and resuspended at 1.5×10^6 cells/ml in KRB buffer plus sulfinpyrazone; 3 ml of this cell suspension were added to each of four quartz cuvettes in a Perkin-Elmer LS-5 spectrofluorimeter. Sedimentation of the cell suspension was prevented by magnetic stirrers in the cuvettes; cuvette temperature was maintained at 37° with a heated cuvette holder. Excitation and emission wavelengths were 340/380 and 510 nm, respectively. Illustrations were made using the data obtained at a single excitation wavelength, 340 nm, but in all protocols experiments were also performed using the 380-nm excitation wavelength. Details of the calculation of $[Ca^{2+}]_i$ were set out in a recent paper from this laboratory (16).

Bis-oxonol fluorescence measurement of membrane potential. Membrane potential was monitored using the fluorescent dye bis-oxonol. Cells were prepared using the procedure outlined above. Dispersed single cells were suspended at 1×10^6 cells/ml in RPMI 1640 medium with 5% fetal bovine serum and 10 mM HEPES. The cells were centrifuged and resuspended in KRB buffer with 100 nM bis-oxonol; gelatin was substituted for 0.1% bovine serum albumin. Three milliliters of the cell suspension were added to each of four quartz cuvettes in a Perkin-Elmer LS-5 spectrofluorimeter. The cell suspension was continuously stirred and allowed to equilibrate in the fluorimeter chamber (maintained at 37°) until the fluorescence signal stabilized (typically 10 min). Excitation and emission wavelengths were 540 and 580 nm, respectively. Gramicidin at 3 μg/ml was added at the end of each trial to determine the maximal membrane depolarization.

Electrophysiological measurement. Before being placed in a 300-μl perifusion chamber, coverslips of cells were preincubated at room temperature (21–23°) for 15 min, in an extracellular buffer that contained 140 mM NaCl, 5 mM KCl, 2 mM $CaCl_2$, 1.1 mM $MgCl_2$, 10 mM HEPES, and 100 μM glucose, with the pH adjusted to 7.4 with NaOH.

Measurement of whole-cell calcium currents. A modification of the nystatin-permeabilized patch, whole-cell, voltage-clamp method was used to measure calcium current (35), with nystatin added to the pipette solution at a final concentration of 250 μg/ml (0.25% dimethylsulfoxide). The extracellular buffer was replaced with a K^+-free, high-Ca^{2+} buffer that contained 110 mM NaCl, 5 mM CsCl, 20 mM $CaCl_2$, and 10 mM HEPES, with the pH adjusted to 7.4 with NaOH; the pipette solution contained 10 mM CsCl, 90 mM $CsSO_4$, 10 mM EGTA, 1 mM $CaCl_2$, and 10 mM HEPES, with the pH adjusted to 7.4 with CsOH. For whole-cell and single-channel experiments, patch pipets were fabricated from Garner glass type 7052 (Garner Glass Co., Claremont, CA) and coated with Sylgard; tip resistances ranged from 3 to 8 MΩ. For measurement of whole-cell calcium currents the pClamp program Clampex (Axon Instruments, Foster City, CA) was used to command the membrane potential to −60 mV and to generate current-voltage plots by stepping (in 10-mV increments) from −50 to +50 mV for 400 msec, after a 200-msec step to −100 mV. Temporal responses to mastoparan were monitored by stepping from the holding potential to +10 mV every 30 sec. Data were acquired via a List EPC-7 amplifier (List Medical, Darmstadt, Germany) and an Axolab-1 (Axon Instruments) interface to an IBM PC-XT computer and were analyzed by using the pClamp program Clampfit to measure the average current during the final 50 msec of each depolarizing step.

Measurement of K(ATP) channel activity. For measurement of K(ATP) channel activity the extracellular buffer was retained in cell-attached patch and excised outside-out patch experiments but was replaced with an intracellular buffer before patch excision in inside-out patch experiments. The intracellular buffer contained 145 mM KCl, 1 mM $CaCl_2$, 1 mM $MgCl_2$, 10 mM EGTA, and 10 mM HEPES, with the pH adjusted to 7.25 with KOH, and unless otherwise stated was augmented with 10–1000 μM ATP and 10 μM GTP when it was bathing the inner side of the excised membrane patches. This buffer, without added nucleotides, was used in the pipette in all single-channel experiments. An Axopatch 1D patch-clamp amplifier (Axon Instruments) was used to obtain the data, which were filtered at 5 kHz and recorded on Beta videotape via a digital audio processor. Analog single-channel data output from the tape was acquired (at a rate of 2–4 kHz) onto the fixed disk of a New Technologies 386/25 MHz computer, via an Axon Instruments TL1/125 DMA interface, using the Axon Instruments program Fetchex. For Figs. 7–13, channel activity was calculated as the product NP_o (where N is the maximum number of channel levels observed in the patch and P_o is the single-channel open probability) from sequential 15-sec data blocks, using the Channel Analysis Program suite (RC Electronics, Goleta, CA). Where mean and standard deviation values are given, they were obtained from at least 2 min (eight blocks) of data. The

majority of chemicals for both electrophysiology and fluorescence studies were obtained from Sigma; bis-oxonol was from Molecular Probes (Eugene, OR) and nitrendipene from Research Biochemicals (Natick, MA).

Results

Effect of mastoparan on $[Ca^{2+}]_i$. Fig. 1 illustrates fura-2 fluorescence in suspensions of RINm5F cells. Mastoparan at 3 μM caused a small increase of $[Ca^{2+}]_i$, which subsided to a level slightly but consistently above basal levels. At 10 μM it caused a well defined initial peak of $[Ca^{2+}]_i$ (in this case about 90 nM above basal levels), followed by a plateau (about 50 nM above basal levels). Similar results were obtained in five different experiments. Using 10 μM mastoparan, peak and steady state values measured 2 min after mastoparan addition were significantly greater than controls ($p < 0.05$) in all experiments, in agreement with a previous report from this laboratory (16). When voltage-dependent calcium channel activity was blocked with 10 μM verapamil, the initial transient response to 3 μM mastoparan was similar to control but the sustained phase was eliminated. The rise in $[Ca^{2+}]_i$ caused by 10 μM mastoparan exhibited similar suppression, with a minor reduction in the initial peak and a pronounced reduction in the sustained plateau value.

Mastoparan increased $[Ca^{2+}]_i$ in HIT cells (Fig. 2) with lower peptide sensitivity and a different profile of response. At 5 and 15 μM mastoparan caused a monophasic increase, as shown in Fig. 2, a and b. This response was suppressed in cells pretreated with 10 μM verapamil (Fig. 2c). In the experiment shown in Fig. 2b, $[Ca^{2+}]_i$ was increased by about 100 nM after 2 min in the presence of 15 μM mastoparan; verapamil reduced this rise by 80% (Fig. 2c). Similar responses were seen in four other experiments.

When different types of organic calcium channel blocker were used, comparable results were obtained. Fig. 3 illustrates the effect of 5 μM mastoparan on $[Ca^{2+}]_i$ in RINm5F cells in the absence (Fig. 3a) and presence of 10 μM diltiazem (Fig. 3b) or nitrendipene (Fig. 3c). Diltiazem reduced the mastoparan-induced rise in $[Ca^{2+}]_i$ by 55%. The quenching effect of nitrendipene on the fura-2 signal prevented quantitation of its effect. It is clear, however, that nitrendipene also reduced the mastoparan-induced rise in $[Ca^{2+}]_i$.

To assess the extent of suppression of voltage-dependent calcium channel activity by these channel blockers, experiments were performed in which cells were depolarized with 25 mM KCl in the absence and presence of channel blockers. Data obtained in the same experiment as that shown in Fig. 3, a-c, are shown in Fig. 3, d-f. Potassium depolarization elicited a rapid rise and peak in $[Ca^{2+}]_i$, which declined slowly (Fig. 3d); after 2 min in the presence of high KCl, $[Ca^{2+}]_i$ was about 75 nM above basal levels. A similar challenge in the presence of 10 μM diltiazem (Fig. 3e) or nitrendipene (Fig. 3f) elicited rapid and transient increases in $[Ca^{2+}]_i$, which, in the case of diltiazem, declined to remain 15 nM above the basal level, an 80% reduction of the KCl-stimulated rise in $[Ca^{2+}]_i$. Similar inhibition was observed in three other experiments with diltiazem. These data indicate that diltiazem reduces but does not fully suppress voltage-dependent calcium channel activity in these cells. Similar suppression of KCl-stimulated $[Ca^{2+}]_i$ elevation was observed using 10 μM verapamil (73% and 78% reduction in two experiments) (data not shown). The response in the presence of nitrendipene indicated nearly complete suppression of the KCl-stimulated $[Ca^{2+}]_i$ rise, but this was not quantitated.

It is evident from these data that extracellular calcium entering the cells via voltage-dependent calcium channels is

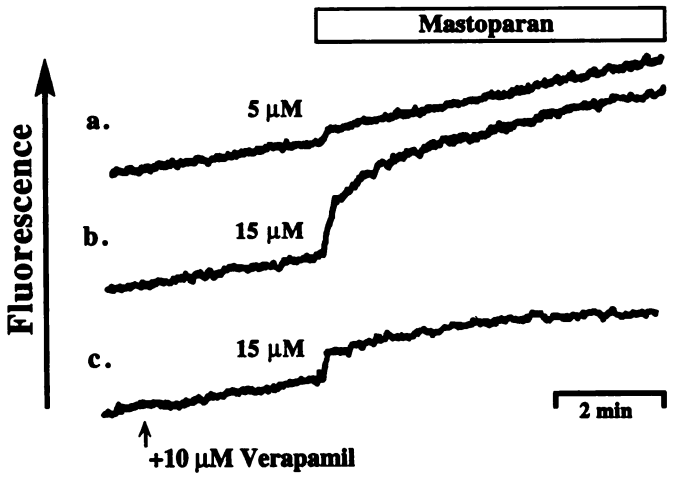

Fig. 2. Fura-2 measurement of $[Ca^{2+}]_i$ in HIT cells in response to mastoparan. Cells were loaded with fura-2 and transferred to cuvettes at a density of 1.5×10^6 cells/ml. Changes of $[Ca^{2+}]_i$ in response to 5 or 15 μM mastoparan were monitored using excitation and emission wavelengths of 340 and 510 nm, respectively, in the absence (a and b) and presence (c) of 10 μM verapamil. *Box above the traces*, periods during which mastoparan was present. *Arrow beneath the trace in c*, addition of verpamil. The data were obtained in the same experiment and are representative of those obtained in five experiments.

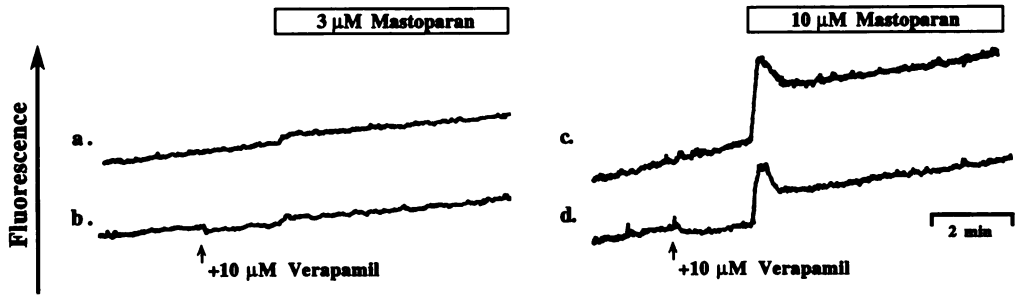

Fig. 1. Fura-2 measurement of $[Ca^{2+}]_i$ in RINm5F cells in response to mastoparan. Cells were loaded with fura-2 and transferred to cuvettes at a density of 1.5×10^6 cells/ml. Changes of $[Ca^{2+}]_i$ in response to 3 μM (a and b) or 10 μM (c and d) mastoparan (*boxes above the traces*) were monitored using excitation and emission wavelengths of 340 and 510 nm, respectively, in the absence (a and c) and presence (b and d) of 10 μM verapamil (*arrows below the traces*). The data were obtained in the same experiment and are representative of those obtained in five experiments.

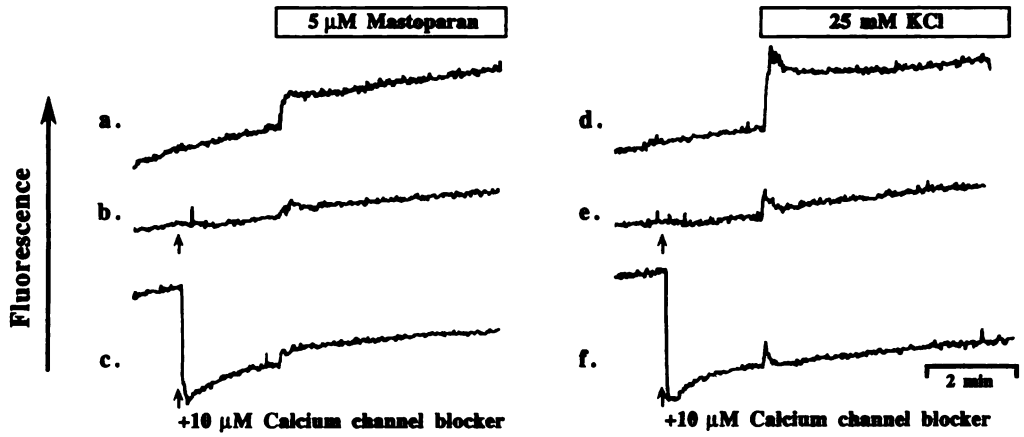

Fig. 3. Fura-2 measurement of $[Ca^{2+}]_i$ in RINm5F cells in response to mastoparan and KCl depolarization and effects of calcium channel blockers. RINm5F cells were challenged with 5 μM mastoparan (a-c) or 25 mM KCl (d-f), in the absence of calcium channel blockers (a and d) or in the presence of 10 μM diltiazem (b and e) or nitrendipene (c and f). *Boxes above the traces*, periods during which mastoparan or elevated KCl was present. *Arrows beneath the traces*, addition of diltiazem (b and e) or nitrendipene (c and f). The data were obtained in the same experiment and are representative of those obtained in three experiments.

largely responsible for the mastoparan-induced rise in $[Ca^{2+}]_i$. This proposal was further investigated by measurement of the response to mastoparan when calcium channel activity was strongly stimulated as a result of cell depolarization by high glucose concentrations, the sulfonylurea glyburide, or combinations of these treatments. Data obtained in the presence of 0.2 mM glucose (Fig. 4a), which has little effect on the HIT or RINm5F cell membrane potential (36), were compared with those obtained in the presence of 10 μM glyburide (Fig. 4b). It is clear that the response of the HIT cells to 15 μM mastoparan was greatly reduced in the presence of the sulfonylurea. Similarly, the response to 15 μM mastoparan was much reduced if the peptide was added in the presence of 20 mM glucose (Fig. 4, a and c) or 20 mM glucose plus glyburide (Fig. 4d). These data are consistent with the proposal that the enhancement of voltage-dependent calcium channel activity evoked by mastoparan is mediated via cell depolarization, rather than an effect of the venom on calcium channel activity *per se*.

Effect of mastoparan on voltage-dependent calcium channel activity. To investigate more directly whether mastoparan affects the behavior of voltage-dependent calcium channels, whole-cell calcium currents were measured under voltage-clamp conditions, using the nystatin-permeabilized patch method (35). Current-voltage plots were constructed before addition of 10 μM mastoparan and at 3-min intervals after addition. Between the full current-voltage plot determinations, depolarizing pulses to +10 mV were applied at 30-sec intervals to monitor temporal effects of the peptide. In 12 experiments of this type there was no consistent effect of 10 μM mastoparan on either the voltage dependence or magnitude of the calcium currents (data not shown).

Effect of mastoparan on membrane potential. Because no direct effect of mastoparan on calcium current was apparent, the proposal that the peptide acts indirectly on voltage-dependent calcium channels via cell depolarization was further tested using the fluorimetric membrane potential indicator bis-oxonol. Data representative of three to six experiments at each mastoparan concentration with both cell types demonstrate the response of RINm5F cells (Fig. 5, a and b) and HIT cells (Fig. 5, c and d) to 3 and 10 μM mastoparan. In both cell types a clear increase in bis-oxonol fluorescence, indicating depolarization, followed addition of mastoparan. Depolarization commenced immediately after peptide addition and established a steady state value within 2–3 min. Subsequent addition of 3 μg/ml gramicidin collapsed the membrane potential of the cells. When the cells were initially depolarized by addition of either 10 μM glyburide (Fig. 6a) or 20 mM glucose (Fig. 6b), mastoparan had little or no further effect on bis-oxonol fluorescence. Both high glucose concentrations and glyburide depolarize insulin-secreting cells by closure of K(ATP) channels; because mas-

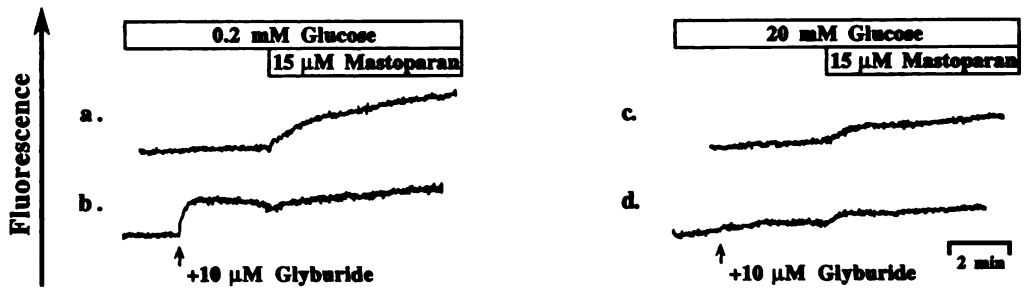

Fig. 4. Fura-2 measurement of $[Ca^{2+}]_i$ in HIT cells in response to mastoparan and modification of the response by glucose and glyburide. HIT cells were challenged with 15 μM mastoparan in the presence of glucose at 0.2 mM (a and b) or 20 mM (c and d). In b and d, 10 μM glyburide was added (*arrows beneath the traces*) 2 min before the mastoparan challenge. The data were obtained in the same experiment and are representative of those obtained in three experiments.

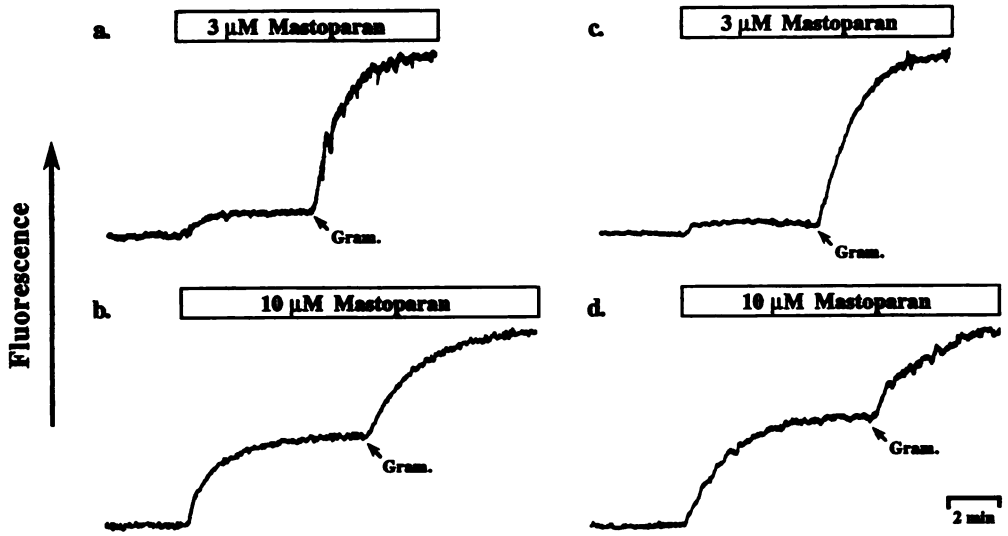

Fig. 5. Bis-oxonol measurement of membrane potential in RINm5F and HIT cells in response to mastoparan. Cells were loaded with the potentiometric dye bis-oxonol and transferred to cuvettes at a density of 1.5 × 10^6/ml. Changes of membrane potential in RINm5F cells (a and b) and HIT cells (c and d) in response to 3 μM (a and c) or 10 μM (b and d) mastoparan were monitored using excitation and emission wavelengths of 540 and 580 nm, respectively. Increases in the fluorescence signal represent cell depolarization. Gramicidin (*Gram.*) was added at 3 μg/ml. The data are representative of those obtained in three to six experiments with each cell type.

toparan did not produce further depolarization, it may be proposed that mastoparan acts via the same mechanism. Control experiments in which mastoparan was added to bis-oxonol-containing buffer in the absence of cells demonstrated that the peptide did not affect the fluorescence of the indicator.

Effect of mastoparan on K(ATP) channel activity in cell-attached patches. Cell-attached patches were used to determine whether mastoparan addition results in suppression of K(ATP) channel activity, as occurs in the presence of nutrient and pharmacological secretagogues and as suggested by the data described above. In both RINm5F and HIT cells in the presence of low (<500 μM) glucose concentrations, with 145 mM K^+ in the pipette and a holding potential of 0 mV, the K(ATP) channel was the only active channel species. It was characterized by its conductance of inward current (55–75 pS), lack of voltage dependence, and inward rectification (34). Channel activity was expressed in terms of the product NP_o; both N, the number of active channels in the patch, and P_o, the open channel probability for the individual channel, were highly variable between patches and this is reflected in the control values of NP_o obtained in this study, which ranged between 0.01 and 1.95; no systematic difference was observed between patches on RINm5F and HIT cells.

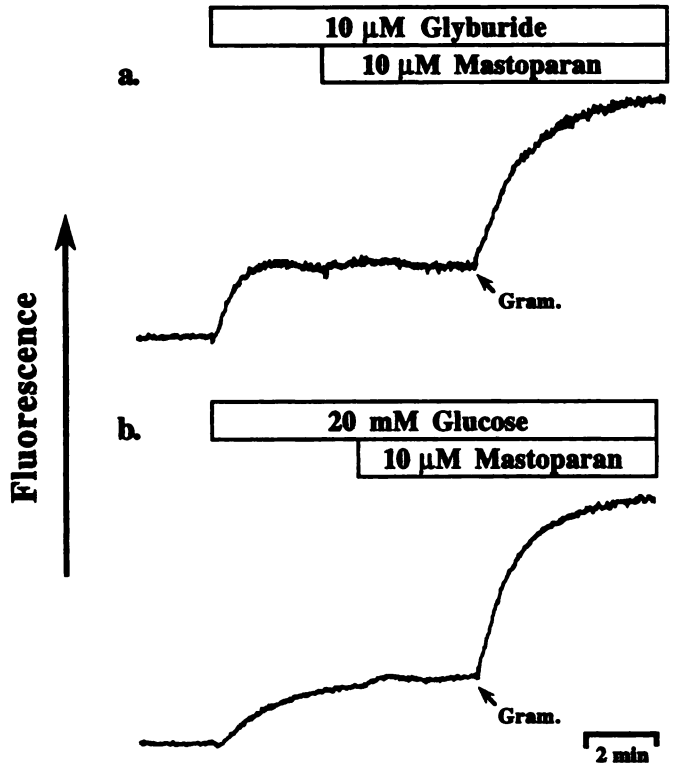

Fig. 6. Bis-oxonol measurement of membrane potential in HIT cells in response to mastoparan and modification of the response by glyburide and glucose. a, Mastoparan was added 3 min after 10 μM glyburide; b, mastoparan was added 4 min after 20 mM glucose. Gramicidin (*Gram.*) was added at 3 μg/ml. The data are representative of those obtained in four experiments.

Mastoparan was added to cell-attached patches at 3–10 μM and its addition was followed by suppression of K(ATP) channel activity. Inhibition of channel activity varied between experiments, from 65 to 93% of control; the interval between mastoparan addition and establishment of the new steady state varied between 3 and 9 min. Neither the maximal degree of channel inhibition nor the time to establish the steady state response to mastoparan was clearly concentration dependent. Recovery of channel activity after removal of mastoparan from the bath was limited, exceeding 60% in only two of 14 mastoparan challenges. In two other experiments, mastoparan at 3 and 5 μM had no demonstrable effect on K(ATP) channel activity in cell-attached patches. The K(ATP) channel response to 10 μM mastoparan in a HIT cell is illustrated in Fig. 7. As in succeeding figures, Fig. 7a summarizes the experimental data, in terms of NP_o, for consecutive 15-sec intervals, illustrating the dynamics and the extent of channel inhibition due to mastoparan. Fig. 7b shows single-channel data from the intervals labeled I and II in Fig. 7a. In this experiment, 10 μM mastoparan progressively reduced K(ATP) channel activity from a control value of 1.9 ± 0.4 (mean ± standard deviation of data points before mastoparan addition) to 0.4 ± 0.03 (data from last 2 min in the presence of mastoparan), an 80% reduction of activity, in 8 min. Recovery of activity reached only 0.78 (40% of initial control) 15 min after mastoparan removal (data not shown).

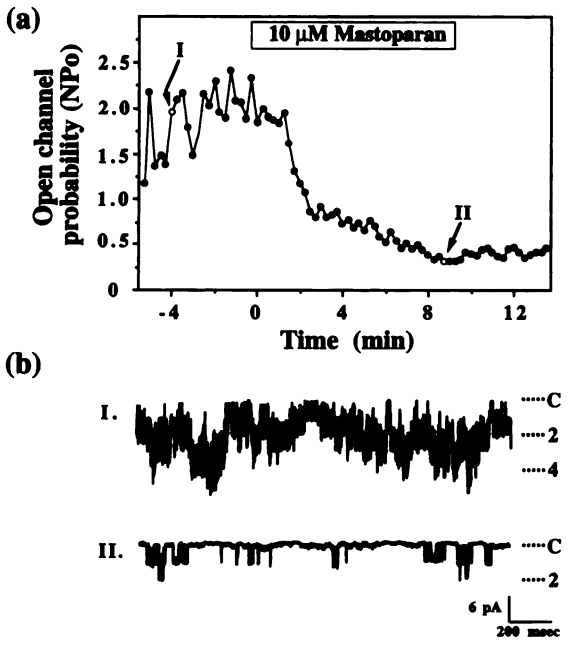

Fig. 7. Cell-attached patch measurement of K(ATP) channel activity in HIT cells. a, Channel activity calculated as NP_o during successive 15-sec intervals. b, Data samples taken from the records indicated in a, representing initial control activity (*I*) and activity in the presence of 10 μM mastoparan (*II*); downward deflections of the current traces indicate inward potassium currents. *Dashed lines to the right of the traces*, closed level (*C*) and open channel levels for two (*2*) and four (*4*) channels. This response was seen in 14 patches.

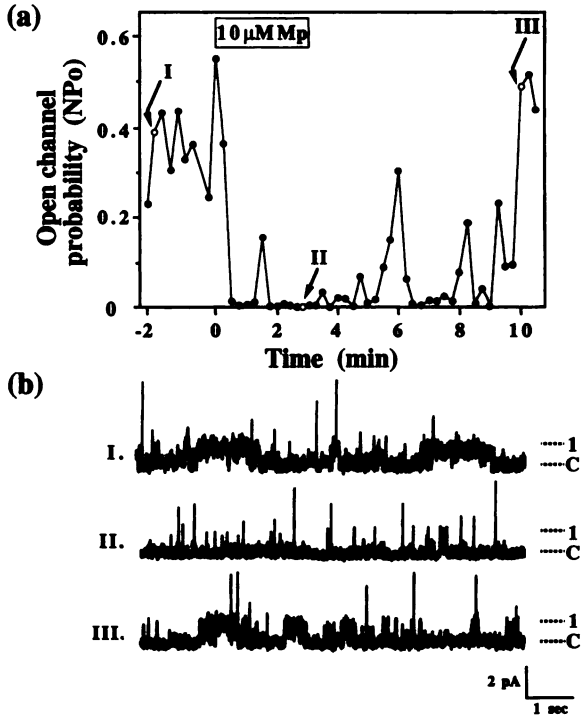

Fig. 8. Excised, outside-out patch measurement of the effect of mastoparan (*Mp*) on K(ATP) channel activity in RINm5F cells. a, Channel activity calculated as NP_o during successive 15-sec intervals. b, Data samples taken from the records indicated in a, representing initial control activity (*I*), activity in the presence of 10 μM mastoparan (*II*), and activity after removal of the peptide (*III*); upward deflections of the current traces indicate outward potassium currents. *Dashed lines to the right of the traces*, closed level (*C*) and single-channel open level (*1*). The rapid large channel openings represent activity of the maxi-K^+ channel. Only one of the 11 patches investigated failed to exhibit recovery from mastoparan-mediated K(ATP) channel inhibition.

Effect of mastoparan on K(ATP) channel activity in excised outside-out patches. To determine whether mastoparan-induced K(ATP) channel inhibition is membrane delimited, additional experiments were carried out using excised membrane patches. Patches were excised in the outside-out configuration from RINm5F and HIT cells, with 100-1000 μM ATP and 10 μM GTP in the intracellular buffer in the pipette. The outside of the patch was exposed to extracellular buffer with no holding potential applied; under these conditions the K(ATP) channel was the dominant channel species, with a single-channel current of 1.5–2 pA. As in cell-attached patches, control activity varied greatly between patch preparations, with NP_o values ranging from 0.07 to 0.98. Mastoparan was added to the bath (i.e., the outer face of the membrane) at 1–10 μM after observation of at least 5 min of steady state activity. At 1 μM, mastoparan reduced K(ATP) channel activity by about 65%, whereas 3 and 10 μM mastoparan caused reductions of 70–99%. With 1 μM mastoparan a new steady state was established 8–9 min after addition, whereas at 3 and 10 μM this interval ranged from <1 min to 7 min. Complete reversibility of the inhibitory effect of mastoparan followed washout in seven patches, with control activity being recovered 2–10 min after removal of the peptide. In one patch of 11, no recovery was observed. An experiment showing the response to 10 μM is summarized in Fig. 8a, with illustrative data obtained before addition of mastoparan (Fig. 8b, *I*), in the presence of the peptide (Fig. 8b, *II*), and after removal of the peptide (Fig. 8b, *III*) being shown in Fig. 8b. In this experiment, addition of 10 μM mastoparan was followed by a rapid fall in K(ATP) channel activity from a control NP_o value of 0.34 ± 0.07 to 0.07 ± 0.04 in about 2 min. Recovery of channel activity followed removal of the peptide; control activity in this case was restored 7 min after removal of mastoparan.

To assess whether mastoparan and sulfonylureas interact in their control of the K(ATP) channel, experiments were carried out in which the two agents were added to excised outside-out patches. The result of one such experiment is shown in Fig. 9 and demonstrates that the reduction of channel activity after addition of 3 μM mastoparan was enhanced by subsequent addition of 20 μM tolbutamide. These data indicate that the two types of inhibitor act on the same channel and that neither impedes the ability of the other to reach its site of action.

Effect of mastoparan on K(ATP) channel activity in excised inside-out patches in the presence of GTP. In excised inside-out patches from both RINm5F and HIT cells exposed to symmetrical 145 mM K^+ buffer, with 10 μM ATP and 10 μM GTP in the bath and a patch potential of −40 to −70 mV, the K(ATP) channel was usually the only potassium channel species observed and was identified by its conductance, lack of voltage dependence, and characteristic inward rectification (34). Channel activity was monitored to ensure that a steady state had been maintained for at least 5 min before mastoparan was added. As observed in outside-out patches, addition of 1–10 μM mastoparan to the bath (i.e., the inner face of the membrane) was followed by a decrease of K(ATP) channel activity. At low concentrations of mastoparan, the channel activity declined slowly. For example, in the

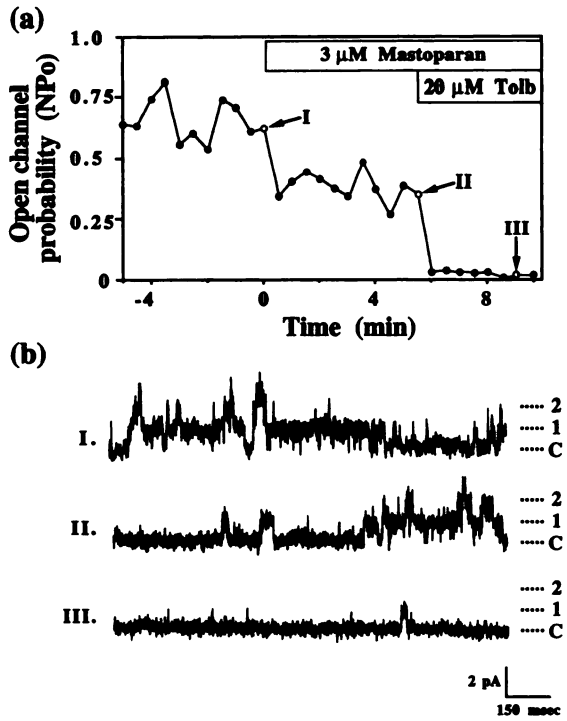

Fig. 9. Excised, outside-out patch measurement of the effect of mastoparan on K(ATP) channel activity in HIT cells. a, Channel activity calculated as NP_o during successive 30-sec intervals. b, Data samples taken from the records indicated in a, representing initial control activity (*I*), activity in the presence of 3 μM mastoparan (*II*), and activity in the presence of 3 μM mastoparan plus 20 μM tolbutamide (*Tolb*) (*III*); upward deflections of the current traces indicate outward potassium currents. *Dashed lines to the right of the traces*, closed level (*C*) and two open channel levels (*1* and *2*). These data are representative of data obtained in five experiments.

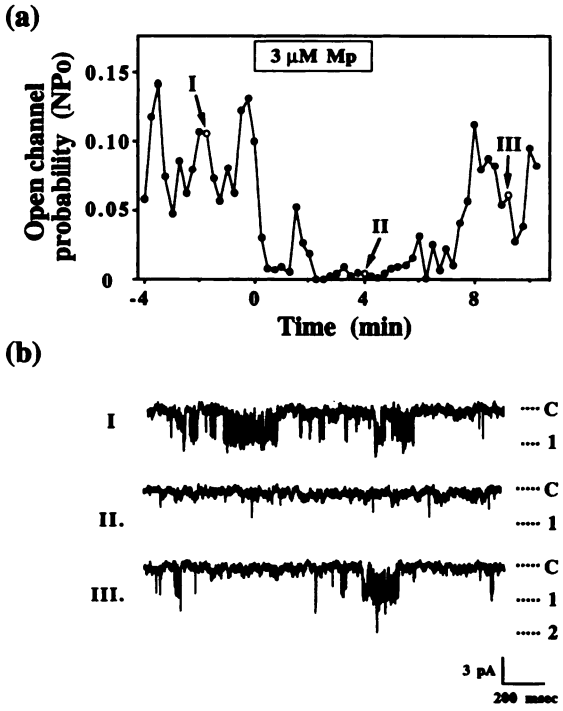

Fig. 10. Excised, inside-out patch measurement of the effect of mastoparan (*Mp*) on K(ATP) channel activity in HIT cells, in the presence of 10 μM GTP. a, Channel activity calculated as NP_o during successive 15-sec intervals. b, Data samples taken from the records indicated in a, representing initial control activity (*I*), activity in the presence of 3 μM mastoparan (*II*), and activity after removal of the peptide (*III*); downward deflections of the current traces indicate inward potassium currents. *Dashed lines to the right of the traces*, closed level (*C*) and open levels of two channels (*1* and *2*). Recovery of activity was observed in eight of 11 experiments after removal of mastoparan.

presence of 1 μM mastoparan up to 7 min elapsed before the new steady state was established, whereas at concentrations from 3 to 10 μM a new steady state level was observed within 2–4 min of addition. This is illustrated in Fig. 10; addition of 3 μM mastoparan was followed immediately by a decline in K(ATP) channel activity, from the average control level of 0.09 ± 0.03 to <0.01, within 3 min; a similar interval preceded recovery after removal of the peptide. Recovery occurred in eight of 11 inside-out patch experiments, with activity returning to levels comparable to control values in six of these, in 3–10 min. Data representing channel activity under control conditions (Fig. 10b, *I*), the response to mastoparan (Fig. 10b, *II*), and recovery (Fig. 10b, *III*) are shown in Fig. 10b.

As with the outside-out patches, addition of tolbutamide in the presence of mastoparan enhanced the reduction of channel activity. Additionally, mastoparan effected a further reduction of channel activity in the presence of low concentrations of tolbutamide (data not shown).

Effect of mastoparan on excised inside-out patches with GTP absent. In planar lipid bilayers and in micelles, mastoparan can enhance guanyl nucleotide exchange on heterotrimeric G proteins (24–26), putatively by mimicking the G protein binding domain motif of G protein-linked receptors and interacting with the carboxyl terminus of the G protein α subunit (26). Because K(ATP) channel activity is affected by heterotrimeric G proteins (37), the possibility of G protein involvement in mastoparan-induced channel inhibition was investigated. Experiments were performed in which excised inside-out patches from both RINm5F and HIT cells were incubated in GTP-free medium for 15–30 min before mastoparan addition. Addition of mastoparan after this interval in the absence of GTP was still followed by suppression of K(ATP) channel activity. In four experiments with HIT cells in which 3 μM mastoparan was added after a 15–30-min incubation in the absence of GTP, steady state channel activity was reduced by 87 ± 13% (versus 82 ± 11% with 10 μM GTP present); a representative experiment is summarized in Fig. 11.

The results of these experiments suggested that mastoparan has a membrane-delimited effect on the K(ATP) channel that is independent of G protein activation. To investigate this possibility further, inside-out patch experiments were carried out in which the patch was excised in the absence of exogenous GTP, and 50–250 μM GDP or GDPβS was subsequently added for a 15–30-min incubation period before mastoparan addition. Addition of 3 μM mastoparan under either of these conditions was accompanied by strong suppression of the K(ATP) channel in patches from both RINm5F and HIT cells. This is illustrated in the experiments summarized in Figs. 12 and 13, which represent experiments performed on patches that had been exposed for 30 min to 250 μM GDP or 250 μM GDPβS, respectively, before addition of 3 μM mastoparan. In these experiments, 3 μM mastoparan addition caused channel activity to be reduced by 85 ± 8% (versus 82

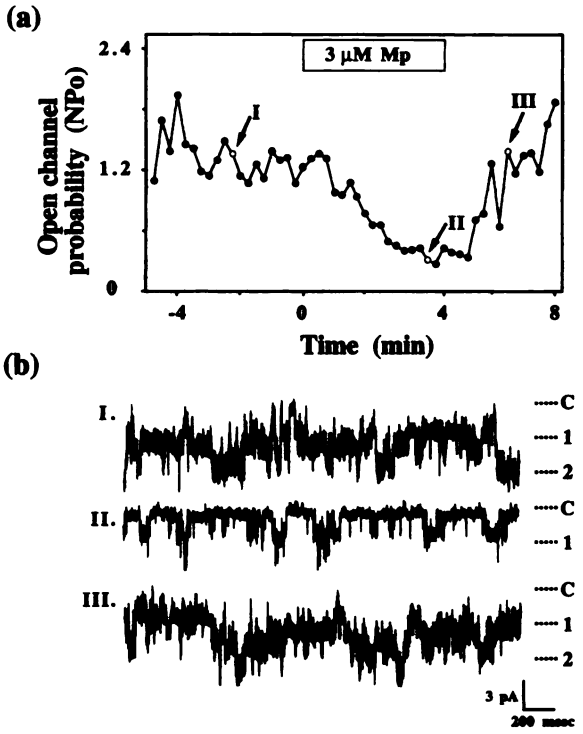

Fig. 11. Excised, inside-out patch measurement of the effect of mastoparan (*Mp*) on K(ATP) channel activity in HIT cells, in the absence of GTP. a, Channel activity calculated as NP_o during successive 15-sec intervals. b, Data samples taken from the records indicated in a, representing initial control activity (*I*), activity in the presence of 3 μM mastoparan (*II*), and activity after removal of the peptide (*III*); downward deflections of the current traces indicate inward potassium currents. *Dashed lines to the right of the traces*, closed level (*C*) and open levels of two channels (*1* and *2*). Data were gathered 30 min after removal of GTP from the bath solution.

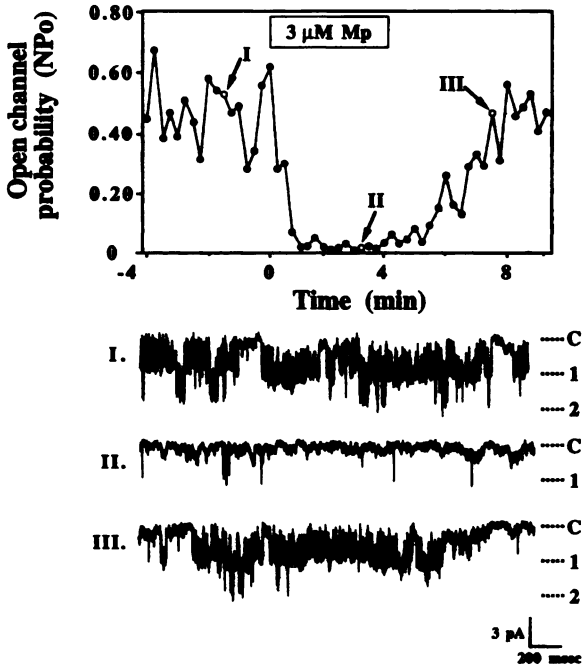

Fig. 12. Excised, inside-out patch measurement of the effect of mastoparan (*Mp*) on K(ATP) channel activity in HIT cells, in the presence of 250 μM GDP. *Upper*, Channel activity calculated as NP_o during successive 15-sec intervals. *Lower*, Data samples taken from the records indicated in a, representing initial control activity (*I*), activity in the presence of 3 μM mastoparan (*II*), and activity after removal of the peptide (*III*); downward deflections of the current traces indicate inward potassium currents. *Dashed lines to the right of the traces*, closed level (*C*) and open levels of two channels (*1* and *2*). Data were gathered after 30 min in the presence of GDP.

± 11% with 10 μM GTP present). From these data it is clear that neither the absence of GTP nor the presence of GDP or GDPβS decreased the suppressive effect of mastoparan on the K(ATP) channels.

Discussion

Nutrient and therapeutic secretagogues increase $[Ca^{2+}]_i$ in insulin-secreting cells largely via cell depolarization and calcium influx through voltage-dependent calcium channels (30); depolarization occurs as a result of closure of K(ATP) channels (32). It was hypothesized that this pathway contributes to the increase of $[Ca^{2+}]_i$ that occurs in the presence of mastoparan.

The observation of mastoparan-induced elevation of $[Ca^{2+}]_i$ confirms recent results from this laboratory using RINm5F cells (16) and demonstrates that mastoparan also induces a rise in $[Ca^{2+}]_i$ in HIT cells, albeit with lower peptide sensitivity. The onset of calcium elevation was rapid in both cell types, commencing within 30 sec of peptide addition and reaching a steady state within the next 1 min. Such a rapid increase in $[Ca^{2+}]_i$ in response to mastoparan has also been described in batch incubations of neutrophils (5), PC-12 cells (8), and alveolar cells (9). At the single-cell level, mastoparan rapidly elicits an oscillatory pattern of increased $[Ca^{2+}]_i$ in pancreatic acinar cells (38).

In two earlier studies on insulin-secreting cells the mastoparan-induced rise in $[Ca^{2+}]_i$ was not reduced by the dihydropyridine nitrendipene at 1 μM (12, 16), although, at least in RINm5F cells, this concentration completely suppressed the sustained elevation of $[Ca^{2+}]_i$ induced by high potassium levels (33). Based on these observations, it was proposed that this $[Ca^{2+}]_i$ increase was independent of calcium influx via voltage-dependent calcium channels (12, 16). However, the demonstration that mastoparan suppresses nitrendipene binding to brain membranes (39) suggested an alternative possibility, i.e., that mastoparan may impede nitrendipene binding to, and blocking of, the voltage-dependent calcium channel. In support of this, the present study showed that calcium channel blockers of both the benzothiazipene (diltiazem) and phenylalkylamine (verapamil) types, which possess different binding sites on the L-type calcium channel (40), caused a significant reduction of the mastoparan-induced $[Ca^{2+}]_i$ elevation (Fig. 3). Furthermore, application of 10 μM nitrendipene, a 10-fold higher concentration than that used previously (12, 16), did inhibit the mastoparan-induced rise in $[Ca^{2+}]_i$. These data implicate calcium influx via voltage-dependent calcium channels as a major component of this response. Clearly, if mastoparan could affect nitrendipene binding to the voltage-dependent calcium channel, then it might also affect calcium channel behavior. This possibility was investigated and discarded, based on the observation that in voltage-clamp experiments mastoparan had no consistent effect on either the magnitude or the voltage dependence of whole-cell calcium currents.

Data obtained using the potentiometric dye bis-oxonol to

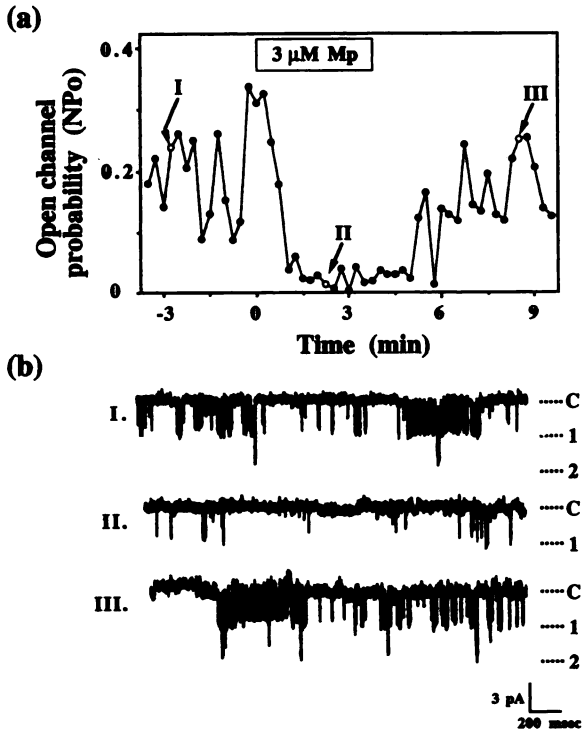

Fig. 13. Excised, inside-out patch measurement of the effect of mastoparan (*Mp*) on K(ATP) channel activity in HIT cells, in the presence of 250 μM GDPβS. a, Channel activity calculated as NP_o during successive 15-sec intervals. b, Data samples taken from the records indicated in a, representing initial control activity (*I*), activity in the presence of 3 μM mastoparan (*II*), and activity after removal of the peptide (*III*); downward deflections of the current traces indicate inward potassium currents. *Dashed lines to the right of the traces*, closed level (*C*) and open levels of two channels (*1* and *2*). Data were gathered after 30 min in the presence of GDPβS.

assess membrane potential in batches of RINm5F and HIT cells were consistent with the hypothesis that mastoparan causes activation of calcium channels by provoking cell depolarization. These data confirmed that depolarization accompanies and may be responsible for activation of voltage-dependent calcium channels and the rise of $[Ca^{2+}]_i$. In support of this, the depolarizing response occurred over the same concentration range as that which provoked elevation of $[Ca^{2+}]_i$, with a similar rapid time course. The finding that bis-oxonol fluorescence was little affected by mastoparan in the presence of either a sulfonylurea or a high concentration of glucose, conditions that greatly reduced the effect of mastoparan on $[Ca^{2+}]_i$, offers further support while also suggesting that the venom acts to suppress K(ATP) channel activity.

The results of cell-attached patch experiments directly implicate reduction of K(ATP) channel activity in the depolarizing response to mastoparan. The same concentration range of mastoparan caused suppression of K(ATP) channel activity, cell depolarization, and elevation of $[Ca^{2+}]_i$. The slower development of responses in cell-attached patches may be expected, because mastoparan was added to the bath and not to the pipette in these experiments. If the effector pathway is membrane delimited, this delay may be ascribed to the interval during which the peptide permeates the membrane to reach the patch circumscribed by the pipette; this may similarly explain the poor reversibility of channel inhibition in this patch configuration after mastoparan removal.

In contrast to the cell-attached patch data, responses to mastoparan in excised outside-out patches, a configuration that more accurately mirrors the mastoparan/membrane relationship pertaining in the secretion studies, were more rapid in onset, although still slower than those observed in fluorimetric studies. Also, in this patch configuration channel inhibition was more readily reversible upon removal of the peptide. These data demonstrate that an inhibitory effect of mastoparan on K(ATP) channel activity occurs via a membrane-delimited pathway; whether, in addition, there is an intracellular mechanism that contributes to K(ATP) channel modulation by mastoparan is not resolved. The data obtained in experiments in which the effects of mastoparan and tolbutamide were tested simultaneously suggest that the effects of these compounds are additive, although the possibility that they act at the same site may not be resolved.

Experiments using inside-out patches yielded results similar to those obtained using outside-out patches. The onset of channel inhibition by mastoparan was more rapid at higher mastoparan concentrations and, as in outside-out patches, was largely reversible. The majority of excised patch experiments were carried out with both ATP and GTP available at the inner side of the membrane. ATP was included to counter channel activity run-down, which occurs when patches are maintained in the complete absence of the nucleotide (41), whereas GTP was included because it was initially considered that the effect of mastoparan may be mediated via its ability to stimulate G protein activity (24–27). However, the inhibitory effect of mastoparan on K(ATP) channel activity persisted in the absence of GTP, as it also persisted in the presence of GDP or GDPβS, suggesting that membrane-delimited inhibition of the K(ATP) channel induced by mastoparan is independent of G proteins. One caveat to this concerns the possible effects of nucleoside diphosphate kinase, a ubiquitous enzyme of which a fraction is membrane bound (42, 43). This enzyme is stimulated by mastoparan over the concentration range of 0.1–10 μM (44) and could, by catalyzing the transfer of the γ-phosphate from ATP to GDP, furnish GTP for mastoparan-induced stimulation of G proteins. However, because nucleoside diphosphate kinase does not affect GDP bound to α subunits of heterotrimeric G proteins (45), the persistence of channel inhibition after a 30-min incubation in the absence of guanine nucleotides suggests that this pathway is not effective.

Mastoparan influences the activity of a number of cellular proteins, some via enhancement of G protein guanyl nucleotide exchange and others directly. Among these are several plasma membrane ion channels, including the calcium- and voltage-sensitive 'maxi'-K^+ channel, which is inhibited by mastoparan in the concentration range of 0.1–10 μM (46), and apical K^+ and Cl^- conductances of Madin-Darby canine kidney cells, which are stimulated by 10 μM mastoparan (47). Both of these responses, inhibitory and stimulatory, are thought to be mediated via the G protein-activating property of mastoparan, whereas calmodulin binding by mastoparan may also affect maxi-K^+ channel activity (46). Higher concentrations of mastoparan rapidly suppress the activity of several ATPases, including the Na^+/K^+-ATPase (48–50), PKC (49, 50), calcium/calmodulin-dependent protein kinase II (49), and myosin light chain kinase (49). In some cases it appears that mastoparan may bind to stimulatory elements in the membrane and prevent their association with these

enzymes. Thus, mastoparan may bind to phosphatidylinositol, which has been implicated as a stimulatory element in the case of the Na^+/K^+-ATPase (48), and phosphatidylserine, which stimulates PKC (49). For calcium/calmodulin-dependent protein kinase II and myosin light chain kinase, it has been suggested that the calmodulin-binding property of mastoparan (22, 23) mediates the inhibitory effect (49).

In view of the data obtained in the presence of GDP and GDPβS, it is unlikely that a G protein mediates K(ATP) channel inhibition induced by mastoparan; therefore, other effector pathways must be considered. In excised RINm5F cell membrane patches this channel is stimulated when PKC activity is enhanced (37); if mastoparan acts to inhibit PKC, then reduced channel activity would be predicted. Activity of the K(ATP) channel is also suppressed by lysophospholipids or unoxygenated arachidonic acid (51, 52), products of phospholipase A_2 action on membrane phospholipids. Either or both of these membrane phospholipid-derived moieties could mediate the effect of mastoparan on the K(ATP) channel, because it has been established that mastoparan induces an increase of phospholipase A_2 activity in a number of different cell types (2, 9, 17) and that phospholipase A_2 activation in HIT cells suppresses K(ATP) channel activity (52). In support of such a mechanism, mastoparan-induced insulin release from rat islets was abolished by inhibition of phospholipase A_2 with bromophenacyl bromide (12). However, in similar studies using RINm5F cells, this effect was not observed when mepacrine was used (16). Neither of these phospholipase A_2 inhibitors is specific, and further study is required to reconcile these observations.

It is possible that mastoparan interacts directly with elements of the membrane, either the channel protein itself or an associated protein, to inhibit the K(ATP) channel. As described above, there are precedents for such modulatory effects of mastoparan on membrane proteins (48–50), as well as for effects of other amphiphiles on K(ATP) channel activity (51, 52).

In conclusion, the present data indicate that mastoparan acts at the level of the plasma membrane to inhibit K(ATP) channels. Channel inhibition, which appears to be G protein independent, underlies depolarization of the cell and consequent activation of voltage-dependent calcium channels. Calcium influx via this pathway represents a major component of the $[Ca^{2+}]_i$ increase observed in the presence of mastoparan. In the case of nutrient secretagogues and the oral hypoglycemic sulfonylureas, this cascade of events is both necessary and sufficient to provoke insulin release. It is perhaps ironic then that, whereas mastoparan provokes these events, its efficacy as a secretagogue probably results from an interaction with a locus in the secretory mechanism that is distal to, and independent of, the rise in $[Ca^{2+}]_i$ investigated in the present study (14, 16).

Acknowledgments

The authors wish to thank Dr. Xue Hong Tao and Ms. Tami Seaman for their assistance with tissue cultures.

References

1. Hirai, Y., T. Yasuhara, H. Yoshida, T. Nakajima, M. Fujino, and C. Kitada. A new mast cell degranulating peptide "mastoparan" in the venom of *Vespula lewisii*. *Chem. Pharm. Bull. (Tokyo)* **27**:1942–1944 (1979).
2. Argiolas, A., and J. J. Pisano. Facilitation of phospholipase A_2 activity by mastoparans, a new class of mast cell degranulating peptides from wasp venom. *J. Biol. Chem.* **258**:13697–13702 (1983).
3. Okano, Y., H. Takagi, T. Tohmatsu, S. Nakashima, Y. Kuroda, K. Saito, and Y. Nozawa. A wasp venom mastoparan-induced polyphosphoinositide breakdown in rat peritoneal mast cells. *FEBS Lett.* **188**:363–366 (1985).
4. Mousli, M., C. Bronner, J.-L. Bueb, E. Tschirhart, J.-P. Gies, and Y. Landry. Activation of rat peritoneal mast cells by substance P and mastoparan. *J. Pharmacol. Exp. Ther.* **250**:329–335 (1989).
5. Perianin, A., and R. Snyderman. Mastoparan, a wasp venom peptide, identifies two discrete mechanisms for elevating cytosolic calcium and inositol triphosphates in human polymorphonuclear leukocytes. *J. Immunol.* **143**:1669–1673 (1989).
6. Kurihara, H., K. Kitajima, T. Senda, H. Fujita, and T. Nakajima. Multigranular exocytosis induced by phospholipase A_2 activators, mellitin and mastoparan, in rat anterior pituitary cells. *Cell Tissue Res.* **243**:311–316 (1986).
7. Wilson, S. P. Effects of mastoparan on catecholamine release from chromaffin cells. *FEBS Lett.* **247**:239–241 (1989).
8. Choi, O. H., W. L. Padgett, and J. W. Daly. Effects of the amphiphilic peptides mellitin and mastoparan on calcium influx, phosphoinositide breakdown and arachidonic acid release in rat pheochromocytoma PC-12 cells. *J. Pharmacol. Exp. Ther.* **260**:369–375 (1992).
9. Joyce-Brady, M., J. B. Rubins, M. P. Panchenko, J. Bernardo, M. P. Steele, L. Kolm, E. R. Simons, and B. F. Dickey. Mechanisms of mastoparan-stimulated surfactant secretion from isolated pulmonary alveolar type 2 cells. *J. Biol. Chem.* **266**:6859–6865 (1991).
10. Ozaki, Y., Y. Matsumoto, Y. Yatomi, M. Higashihara, T. Kariya, and S. Kume. Mastoparan, a wasp venom, activates platelets via pertussis toxin-sensitive GTP-binding proteins. *Biochem. Biophys. Res. Commun.* **170**:779–785 (1990).
11. Wheeler-Jones, C. P. D., T. Saermark, V. V. Kakkar, and K. S. Authi. Mastoparan promotes exocytosis and increases intracellular cyclic AMP in human platelets: evidence for the existence of a G_o-like mechanism. *Biochem. J.* **281**:465–472 (1992).
12. Yokokawa, N., M. Komatsu, T. Takeda, T. Aizawa, and T. Yamada. Mastoparan, a wasp venom, stimulates insulin release by pancreatic islets through pertussis toxin-sensitive GTP-binding proteins. *Biochem. Biophys. Res. Commun.* **158**:712–716 (1989).
13. Komatsu, M., T. Aizawa, N. Yokokawa, Y. Sato, N. Okada, N. Takasu, and T. Yamada. Mastoparan-induced hormone release from rat pancreatic islets. *Endocrinology* **130**:221–228 (1992).
14. Jones, P. M., F. M. Mann, S. J. Persaud, and C. P. D. Wheeler-Jones. Mastoparan stimulates insulin secretion from pancreatic β-cells by effects at a late stage in the secretory pathway. *Mol. Cell. Endocrinol.* **94**:97–103 (1993).
15. Hillaire-Buys, D., M. Mousli, Y. Landry, J. Bockaert, J. A. Fehrentsz, J. Carrette, and B. Rouot. Insulin releasing effects of mastoparan and amphiphilic substance P receptor antagonists on RINm5F insulinoma cells. *Mol. Cell. Biochem.* **109**:133–138 (1992).
16. Komatsu, M., A. M. McDermott, S. L. Gillison, and G. W. G. Sharp. Mastoparan stimulates exocytosis at a Ca^{2+}-independent late site in stimulus-secretion coupling: studies with the RINm5F β-cell line. *J. Biol. Chem.* **268**:23297–23306 (1993).
17. Gil, J., T. Higgins, and E. Rozengurt. Mastoparan, a novel mitogen for Swiss 3T3 cells, stimulates pertussis toxin-sensitive arachidonic acid release without inositol phosphate accumulation. *J. Cell Biol.* **113**:943–950 (1991).
18. Wallace, M. A., and H. R. Carter. Effects of the wasp venom peptide, mastoparan, on a phosphoinositide-specific phospholipase C purified from rabbit brain membranes. *Biochim. Biophys. Acta* **1006**:311–316 (1989).
19. Gusovsky, F., D. G. Soergel, and J. W. Daly. Effects of mastoparan and related peptides on phosphoinositide breakdown in HL-60 cells and cell-free preparations. *Eur. J. Pharmacol.* **206**:309–314 (1991).
20. Nakahata, N., M. T. Abe, I. Matsuoka, and H. X. Nakanishi. Mastoparan inhibits phosphoinositide hydrolysis via pertussis toxin-insensitive G-protein in human astrocytoma cells. *FEBS Lett.* **260**:91–94 (1989).
21. Wojcikiewicz, R. J. H., and S. R. Nahorski. Phosphoinositide hydrolysis in permeabilized SH-SY5Y human neuroblastoma cells is inhibited by mastoparan. *FEBS Lett.* **247**:341–344 (1989).
22. Malencik, D. A., and S. R. Anderson. High affinity binding of the mastoparans by calmodulin. *Biochem. Biophys. Res. Commun.* **114**:50–56 (1983).
23. Barnette, M. S., R. Daly, and B. Weiss. Inhibition of calmodulin activity by insect venoms. *Biochem. Pharmacol.* **32**:2929–2933 (1983).
24. Higashijima, T., S. Uzu, T. Nakajima, and E. M. Ross. Mastoparan, a peptide toxin from wasp venom, mimics receptors by activating GTP-binding regulatory proteins (G-proteins). *J. Biol. Chem.* **263**:6491–6494 (1988).
25. Higashijima, T., J. Burnier, and E. M. Ross. Regulation of G_i and G_o by mastoparan, related amphiphilic peptides, and hydrophobic amines: mechanisms and structural determinants of activity. *J. Biol. Chem.* **265**:14176–14186 (1990).
26. Higashijima, T., and E. M. Ross. Mapping of the mastoparan-binding site on G proteins: cross-linking of [^{125}I-Tyr^3,Cys^{11}]mastoparan to G_o. *J. Biol. Chem.* **266**:12655–12661 (1991).
27. Koch, G., B. Haberman, C. Mohr, I. Just, and K. Aktories. Interaction of

mastoparan with the low molecular mass GTP-binding proteins rho/rac. *FEBS Lett.* **291**:336–340 (1991).
28. Tanimura, A., Y. Matsumoto, and Y. Tojyo. Mastoparan increases membrane permeability in rat parotid cells independently of action on G-proteins. *Biochem. Biophys. Res. Commun.* **177**:802–808 (1991).
29. Katsu, T., K. Sanchika, H. Yamanaka, S. Shinoda, and Y. Fujita. Mechanism of cellular membrane damage induced by mellitin and mastoparan. *Jpn. J. Med. Sci. Biol.* **43**:259–260 (1990).
30. Wollheim, C. B., and G. W. G. Sharp. Regulation of insulin release by calcium. *Physiol. Rev.* **61**:914–973 (1981).
31. Muramatsu, S., S. Terakawa, and T. Kanno. Mastoparan evokes exocytosis without Ca^{2+} movement in adrenal chromaffin cells. *Jpn. J. Physiol.* **43** (Suppl. 1):S109–S113 (1993).
32. Ashcroft, F. M. Adenosine 5′-triphosphate-sensitive potassium channels. *Annu. Rev. Neurosci.* **11**:97–118 (1988).
33. Yaney, G. C., G. A. Stafford, J. D. Henstenberg, G. W. G. Sharp, and G. A. Weiland. Binding of the dihydropyridine calcium channel blocker (+)-[^{3}H]isopropyl-4-(2,1,3-benzoxadiazol-4-yl)-1,4-dihydro-5-methoxy-carbonyl-2,6-dimethyl-3-pyridinecarboxylate (PN200–110) to RINm5F membranes and cells: characterization and functional significance. *J. Pharmacol. Exp. Ther.* **258**:652–662 (1991).
34. Cook, D. L., and C. N. Hales. Intracellular ATP directly blocks K^+ channels in pancreatic β-cells. *Nature (Lond.)* **311**:271–273 (1984).
35. Horn, D. R., and A. J. Marty. Muscarinic activation of ionic currents measured by a new whole-cell recording method. *J. Gen. Physiol.* **92**:145–159 (1988).
36. Eddlestone, G. T., B. Ribalet, and S. Ciani. A comparative study of K channel behavior in β cell lines with different secretory responses to glucose. *J. Membr. Biol.* **109**:123–134 (1989).
37. Ribalet, B., and G. T. Eddlestone. Characterisation of the G-protein coupling of a SRIF receptor to the K(ATP) channel in insulin secreting cells. *J. Physiol. (Lond.)*, in press.
38. Yule, D. I., and J. A. Williams. Mastoparan induces oscillations of cytosolic Ca^{2+} in rat pancreatic acinar cells. *Biochem. Biophys. Res. Commun.* **177**:159–165 (1991).
39. Goldman, M. E., and J. J. Pisano. Inhibition of [^{3}H]nitrendipene binding by phospholipase A_2. *Life Sci.* **37**:1301–1308 (1985).
40. Catterall, W. A., M. J. Seager, and M. Takahashi. Molecular properties of dihydropyridine-sensitive calcium channels in skeletal muscle. *J. Biol. Chem.* **263**:3535–3538 (1988).
41. Findlay, I., and M. J. Dunne. ATP maintains ATP-inhibited K^+ channels in an operational state. *Pfluegers Arch.* **407**:238–240 (1986).
42. Kimura, N., and N. Shimada. Membrane-associated nucleoside diphosphate kinase from rat liver: purification, characterization and comparison with cytosolic enzyme. *J. Biol. Chem.* **263**:4647–4653 (1988).
43. Kowluru, A., and S. A. Metz. Characterization of nucleoside diphosphate kinase activity in human and rodent pancreatic *beta* cells: evidence for its role in the formation of guanosine triphosphate, a permissive factor for nutrient-induced insulin secretion. *Biochemistry* **33**:12495–12503 (1994).
44. Kikkawa, S., K. Takahashi, K.-i. Takahashi, N. Shimada, M. Ui, N. Kimura, and T. Katada. Activation of nucleoside diphosphate kinase by mastoparan, a peptide isolated from wasp venom. *FEBS Lett.* **305**:237–240 (1992).
45. Randazzo, P. A., J. K. Northup, and R. A. Kahn. Regulatory GTP-binding proteins (ADP-ribosylation factor, G_i, RAS) are not activated directly by nucleoside diphosphate kinase. *J. Biol. Chem.* **267**:18182–18189 (1992).
46. Glavinovic, M. I., A. Joshi, and J. M. Trifaro. Mastoparan blockade of currents through Ca^{2+}-activated K^+ channels in bovine chromaffin cells. *Neuroscience* **50**:675–684 (1992).
47. Winter, M. C., M. R. Carson, R. A. Sheldon, and D. M. Shasby. Mastoparan activates apical chloride and potassium conductances, decreases cell volume, and increases permeability of cultured epithelial cell monolayers. *Am. J. Respir. Cell. Mol. Biol.* **6**:583–593 (1992).
48. Eng, S. P., D. L. Clough, and C. S. Lo. Mastoparan inhibits rat renal NaK-ATPase activity. *Life Sci.* **47**:2451–2458 (1990).
49. Raynor, R. L., B. Zheng, and J. F. Kuo. Membrane interactions of amphiphilic polypeptides mastoparan, mellitin, polymixin B, and cardiotoxin: differential inhibition of protein kinase C, Ca^{2+}/calmodulin-dependent kinase II and synaptosomal membrane Na,K-ATPase, and Na^+ pump and differentiation of HL-60 cells. *J. Biol. Chem.* **266**:2753–2758 (1991).
50. Raynor, R. L., Y.-S. Kim, B. Zheng, W. R. Vogler, and J. F. Kuo. Membrane interactions of mastoparan analogues related to their differential effects on protein kinase C, Na,K-ATPase and HL-60 cells. *FEBS Lett.* **307**:275–279 (1992).
51. Kim, D., and R. A. Duff. Regulation of K^+ channels in cardiac myocytes by free fatty acids. *Circ. Res.* **67**:1040–1046 (1990).
52. Eddlestone, G. T. ATP-sensitive K channel modulation by products of PLA_2 action in the HIT insulin secreting cell line. *Am. J. Physiol.* **268**: C181–190 (1995).

Send reprint requests to: Geoffrey T. Eddlestone, Masonic Medical Research Laboratory, 2150 Bleecker Street, Utica, NY 13501–1787.